Electronic Supplementary Material (ESI) for Inorganic Chemistry Frontiers.

Efficient Photocatalytic Hydrogen Evolution of g-C_3N_4/Vs-SnS_2/CdS through Sulfur Vacancies-rich SnS_2 induced Charge Storage Effect

*Fangyuan Xing, Junyan Li, Chengzhi Wang, Shaohua Jin, Haibo Jin and Jingbo Li**

F. Xing, J. Li, C. Wang, S.H. Jin, H.B. Jin, J.Bo. Li

Beijing Key Laboratory of Construction Tailorable Advanced Functional Materials and Green Applications, School of Materials Science and Engineering, Beijing Institute of Technology, Beijing 100081, China

E-mail: lijb@bit.edu.cn

Experimental Section

Photoelectrochemical measurements

The photoelectrochemical performance was evaluated in a standard three-electrode configuration using an electrochemical workstation (CHI660D, Chenhua, China). A platinum sheet as the counter electrode, and an Ag/AgCl reference electrode. The working electrodes were prepared by the following steps: 6 mg sample was mixed with 40 μL nafion and 1mL ethanol by ultrasonic treatment for 10 min to obtain a slurry. Then, the above solution was dropped onto the precleaned 1.5 cm×1 cm ITO glass electrode surface, followed by air-drying before measurement. Na_2SO_4 (0.5 M) solution was used as the electrolyte.

Evaluation of photocatalytic activity

The photocatalytic overall water splitting reaction was carried out in a Pyrex top-irradiation reaction vessel connected to a glass closed gas system (Perfect Light). 3 wt% Pt as co-catalysts were loaded on the photocatalysts by in situ photo-deposition method using H_2PtCl_6. And 50 mg photocatalysts were dispersed in 80 ml distilled water and 20ml triethanolamine. The reaction solution was kept at 10 °C by recirculating cooling water system, then it was evacuated several times to remove air completely. And a 300W Xe lamp was used as the light source. The amounts of gases produced were measured by gas chromatography equipped with a thermal conductive detector (TCD) and a 5 Å molecular sieve column, using argon as the carrier gas.

Characterization

The structure and morphology of the prepared samples were characterized by X-ray

diffraction (XRD, Cu-Ka, X'pert Pro, PANalytical B. V., Almelo, Netherlands), scanning electron micrrroscopy (SEM, HITACHI S-3500N, Japan) and transmission electron microscopy (TEM, FEI Tecnai G2 F20 S-TWIN). UV-vis diffusion reflectance spectra (UV-vis DRS) of the samples were measured by an UV-vis spectrophotometer (HITACHI U-3310, Hitachi Co., JPN) with an integrating sphere assembly, using $BaSO_4$ as the reflectance sample. BET surface area measurements were recorded by H_2O adsorption using a Micrometrics (ASAP2460) surface area analyzer. The electron paramagnetic resonance (EPR) measurement was carried out on a Bruker EMX PLUS spectrometer. The PL was obtained by a FLS1000 system (Edinburgh Instruments, UK). The IR spectra was obtained by the Thermo Scientific Nicolet^{TM} iS^{TM} 50 Spectromoter. The Contact angle test was obtained by JY-82C. The Surface photovoltage (SPV) measurement was carried out on a Surface photovoltage test system (CEL-SPS1000). The transient absorption measurement (TA) was measured by Vitara-Legend Elite-Helios.

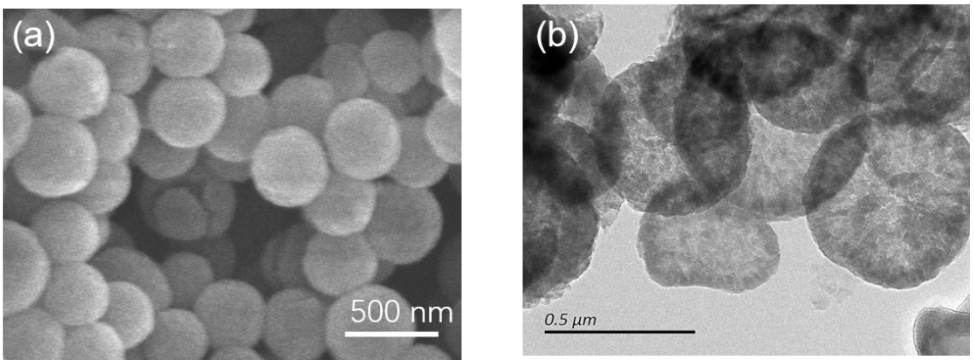

Figure S1 SEM image (a) and TEM image (b) of g-C_3N_4 hollow spheres

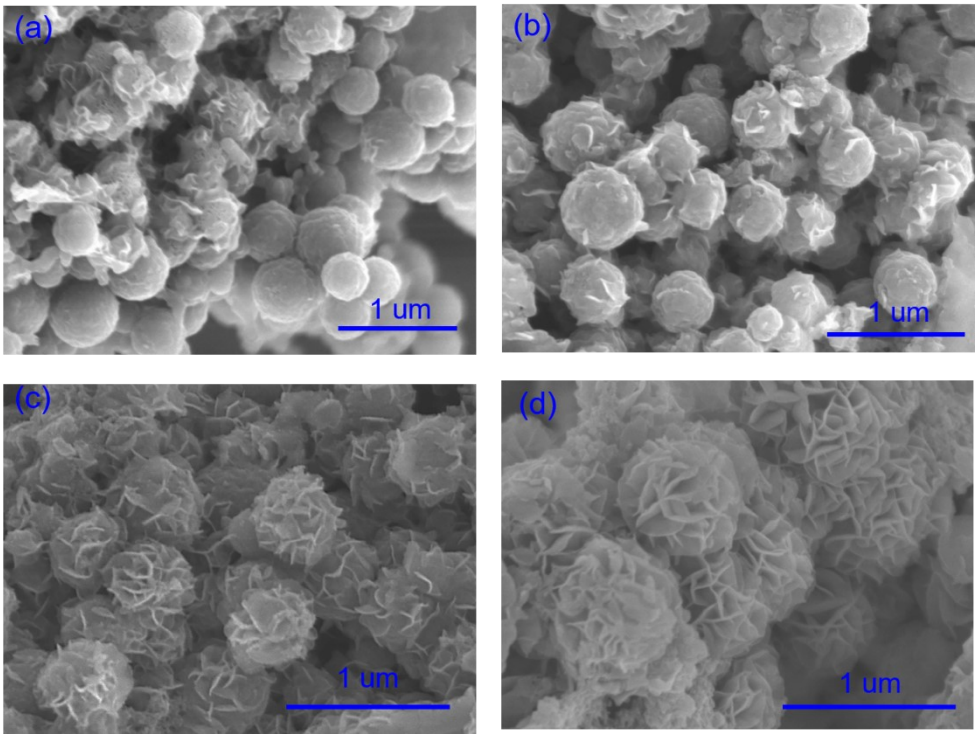

Figure S2 SEM images of g- C_3N_4/SnS_2 loaded with different mass fractions of SnS_2

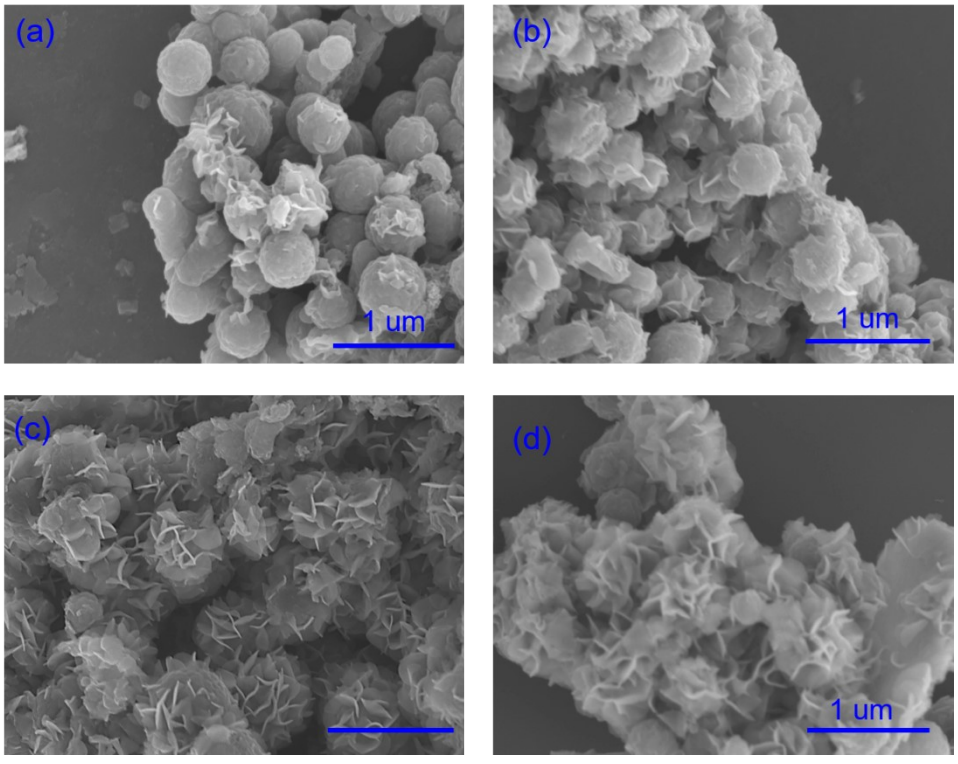

Figure S3 SEM images of g-C_3N_4/Vs-SnS_2 loaded with different mass fractions of SnS_2 (a) 20.3, (b) 25.7, (c) 29.8, and (d) 35.1wt.%

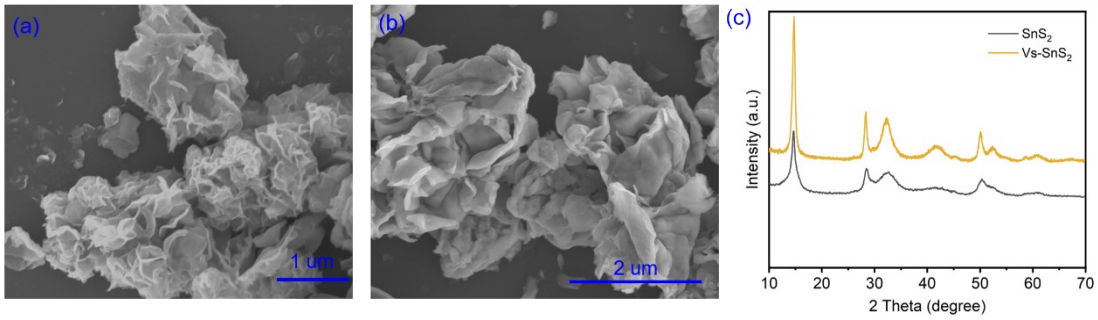

Figure S4 SEM image of SnS_2 (a) and Vs-SnS_2 (b); XRD pattern of SnS_2 and Vs-SnS_2 (c)

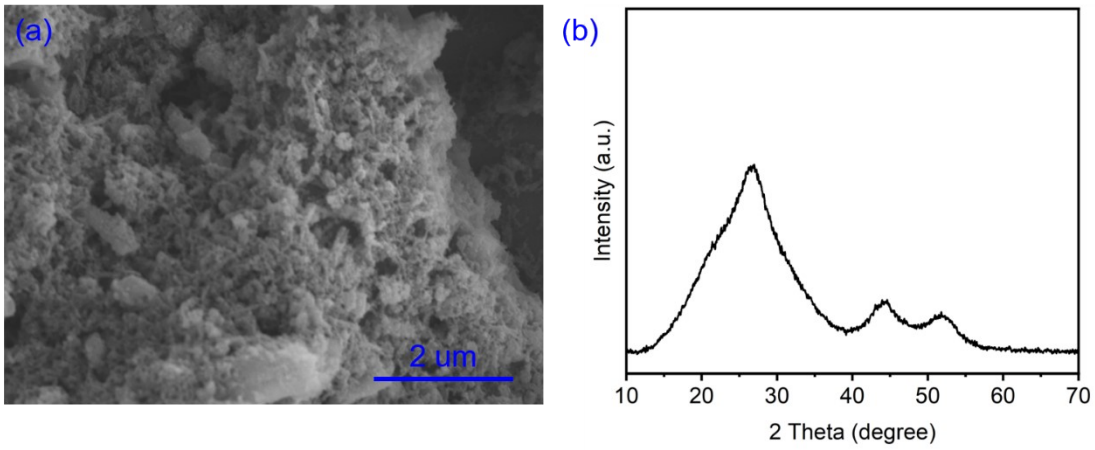

Figure S5 SEM image (a) and XRD patterns (b) of CdS

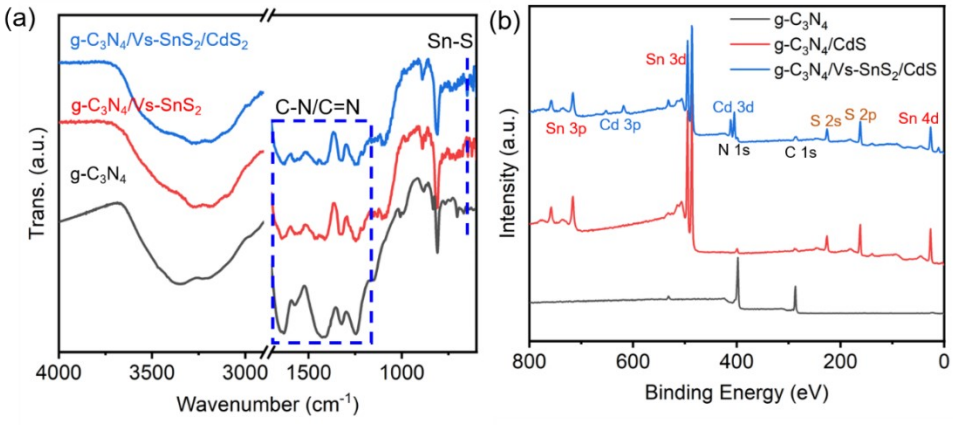

Figure S6 IR spectra (a) and XPS spectra of samples

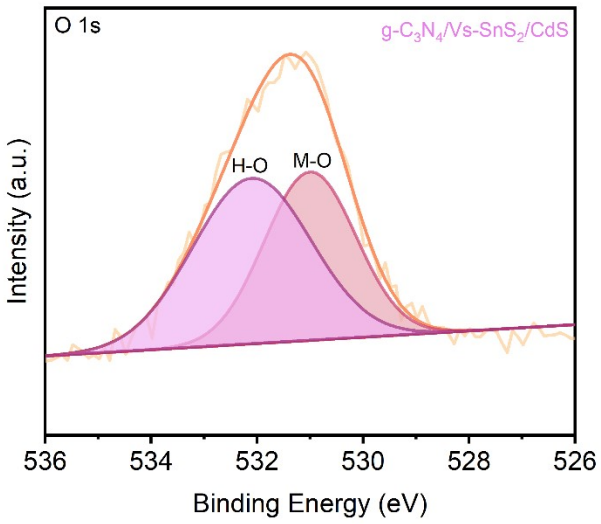

Figure S7 O 1s core-level XPS spectra of g-C_3N_4/Vs -SnS_2/CdS

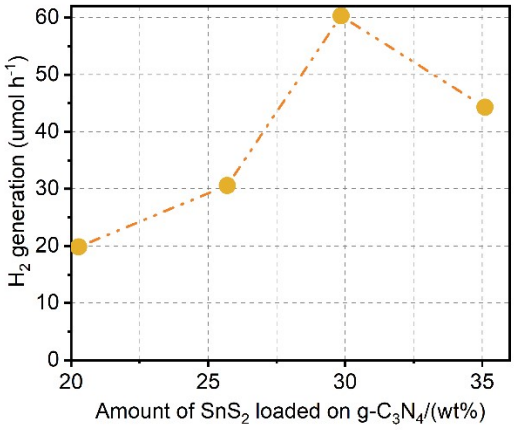

Figure S8 Photocatalytic H_2 evolution rate under visible light irradiation of g-C_3N_4/Vs -SnS_2 photocatalysts with different amount of Vs-SnS_2.

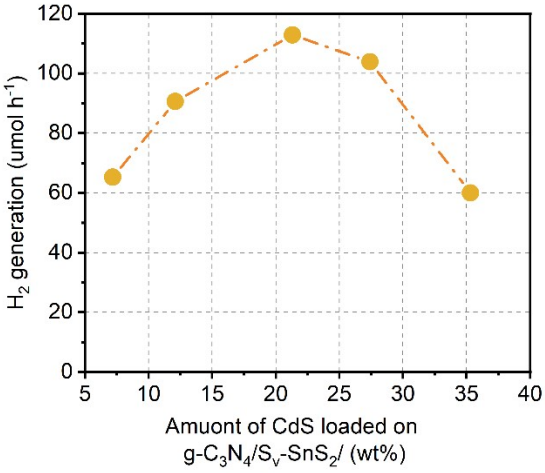

Figure S9 Photocatalytic H_2 evolution rate under visible light irradiation of g-C_3N_4/Vs -SnS_2/CdS photocatalysts with different amount of CdS.

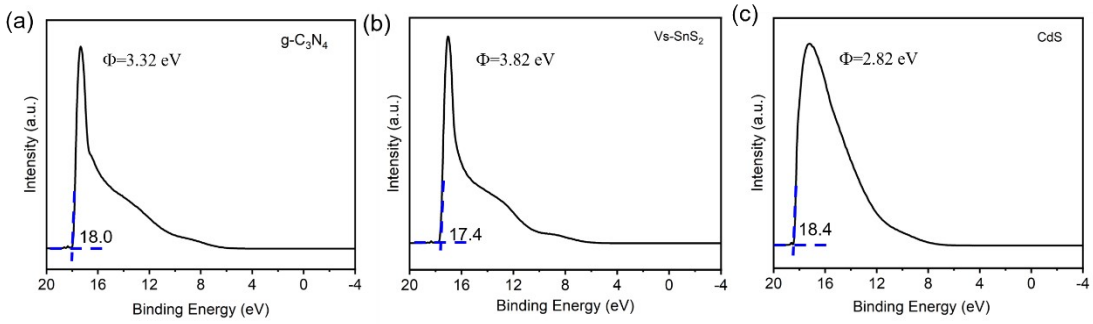

Figure S10 UPS spectra of g-C_3N_4 (a), Vs-SnS_2 (b) and CdS (c)

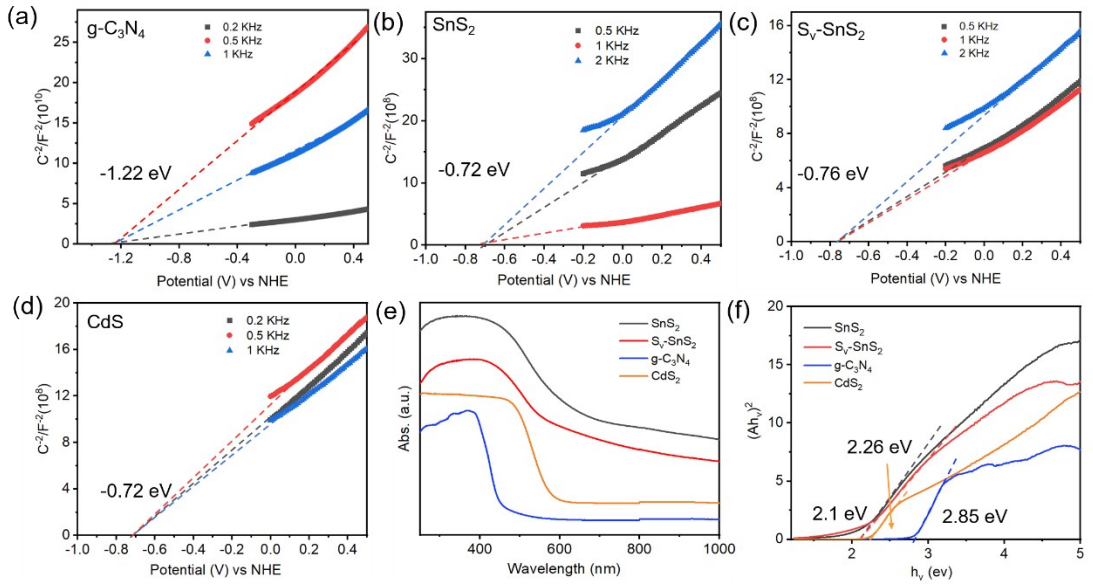

Figure S11 Band structure. Mott-Schottky (M-S) plot of (a) g-C_3N_4, (b) SnS_2, (c) Sv-SnS_2, (d) CdS; UV–vis DRS (e) and Kubelka-Munk function vs. the energy of incident light plots (f) of the samples

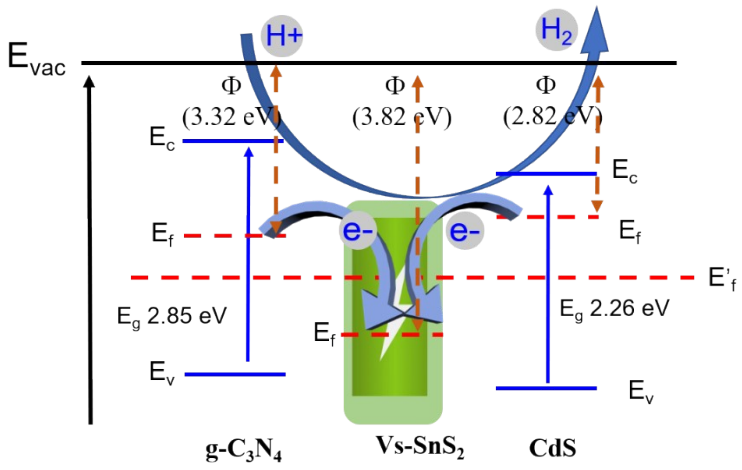

Figure S12 the energy band structure of g-C_3N_4/Vs -SnS_2/CdS

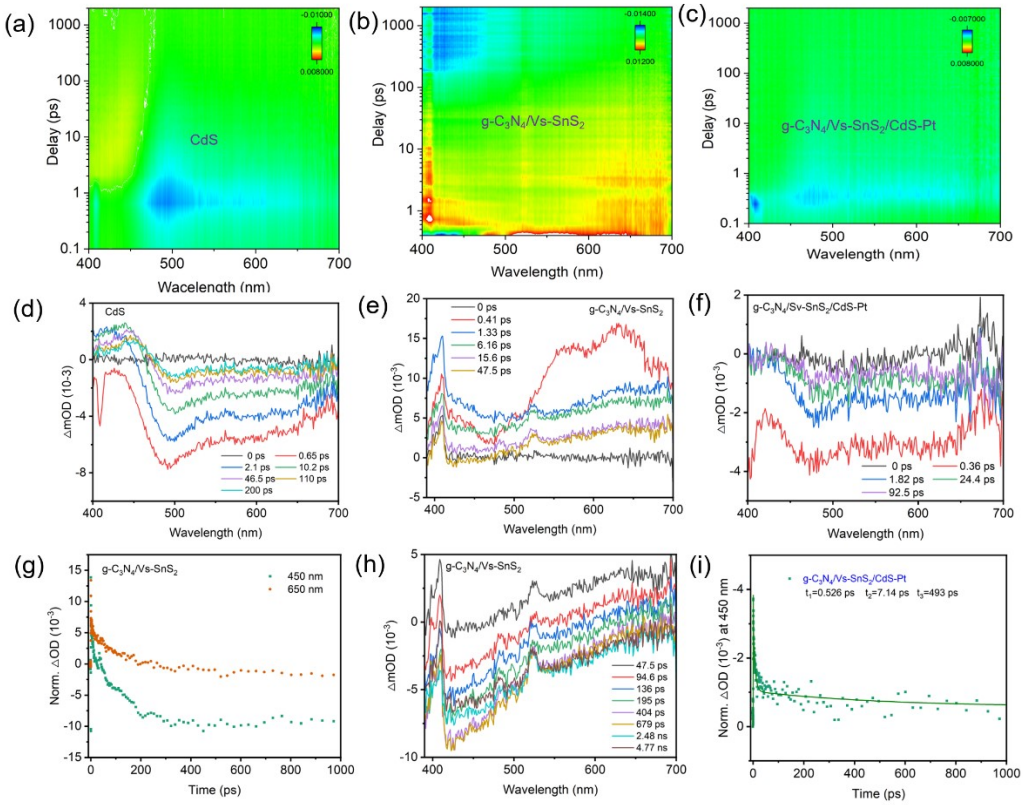

Figure S13 2D mapping TA spectra of (a) CdS, (b) g-C_3N_4/Vs-SnS_2, (c) g-C_3N_4/Vs-SnS_2/CdS-Pt; TA spectra signals of (d) CdS, (e, h) g-C_3N_4/Vs-SnS_2, (f) g-C_3N_4/Vs-SnS_2/CdS-Pt under 360 nm pump; time profiles of normalized TAS for (g) g-C_3N_4/Vs-SnS_2, (i) g-C_3N_4/Vs-SnS_2/CdS-Pt

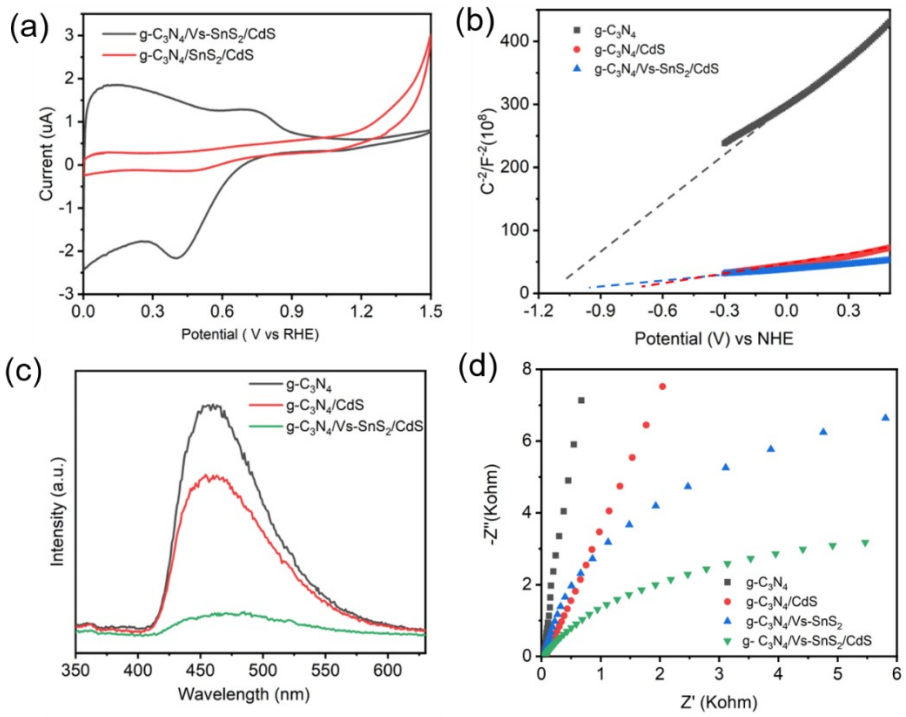

Figure S14 (a) Cyclic voltammetry (CV) curve; (b) Mott–Schottky plots; (c) Photoluminescence spectrum (PL) spectra of the samples; (d) Electrochemical impedance spectra (EIS) of the samples

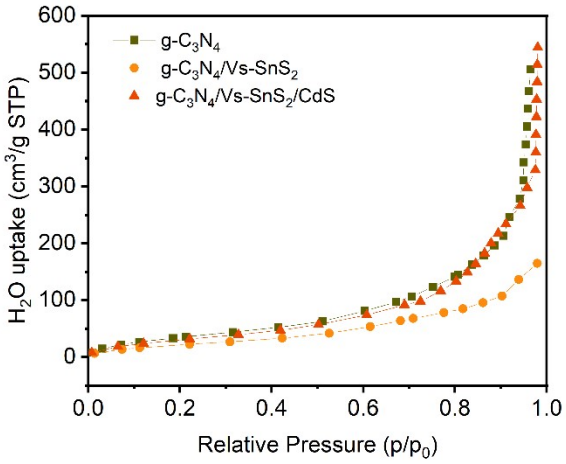

Figure S15 H_2O adsorption isotherm